

## Evidence of Two Forms of Cobaltous Oxide\*

HANG NAM OK† AND JAMES G. MULLEN

*Physics Department, Purdue University, Lafayette, Indiana*

(Received 8 November 1967)

The existence of two forms of cobaltous oxide, CoO(I) and CoO(II), has been established by Mössbauer, x-ray, and chemical techniques. CoO(I) has the NaCl structure as determined by a well-resolved powder x-ray pattern. Its density is measured to be 6.4 g/cm<sup>3</sup> from both x-ray and direct macroscopic experiments. Fe<sup>57</sup> Mössbauer lines in CoO(I), doped with Co<sup>57</sup>, show only Fe<sup>2+</sup> when determined by either the isomer shift or the hyperfine splitting below the Néel temperature. We find a Néel temperature of 288°K, which is 3°K less than the value reported by earlier workers. CoO(I) is completely inert in air at room temperature, and its stoichiometry does not change over time intervals as long as two months. CoO(II) could be prepared at low temperatures only. Form II also had the NaCl structure, but the x-ray line of the powder pattern was very broad. The density of CoO(II) is 3.2 (+1.0, -0.0) g/cm<sup>3</sup>, about half of the value found for CoO(I). CoO(II) shows only Fe<sup>3+</sup> lines in the Mössbauer pattern, with the appropriate isomer shift and hyperfine field. CoO(II) is very reactive with oxygen, at room temperature, although the x-ray pattern is not appreciably altered after oxygen absorption. CoO(II) has a Néel temperature of 270±10°K, slightly less than that of CoO(I), and an effective Mössbauer characteristic temperature of 320°K, substantially less than the 510°K value found for CoO(I). The results of studies of thermally activated transformation of II→I and pressure and quenching experiments are given. CoO(I, II), a mixture of forms I and II, is obtained by the usual chemical recipes. This mixed material was also studied. At low temperature, CoO(I, II) behaves as a simple mixture of I and II, but at temperatures above 200°K there is an interplay between the two forms which is responsible for the observed increase in the relative fraction of Fe<sup>3+</sup> to Fe<sup>2+</sup> observed in the Mössbauer patterns. This interplay is also connected with the shift in the apparent Néel temperature for Fe<sup>3+</sup> in pure form II compared with the value obtained for CoO(I, II). A detailed model is proposed which explains all of the properties observed thus far. The data preclude the possibility of Auger after-effects in cobaltous oxide, as suggested by Wertheim, and they also show that stoichiometry fluctuations are not the principal cause of the observed Fe<sup>3+</sup> Mössbauer line, as was recently claimed by Triftshäuser and Craig.

## I. INTRODUCTION

COBALTOUS oxide, doped with Co<sup>57</sup>, has been the subject of several recent Mössbauer investigations.<sup>1-6</sup> The results of these experiments have shown that the Fe<sup>57</sup> exists in both the divalent and trivalent states in cobaltous oxide.

The existence of the two charge states was interpreted by Wertheim<sup>1</sup> as evidence that the time required to reach electronic charge equilibrium, following the emission of Auger electrons, can be of the order of or greater than the half-life of the first excited state of the nucleus Fe<sup>57</sup> (10<sup>-7</sup> sec). On the basis of Wertheim's results, Pollak<sup>2</sup> concluded that an Auger cascade could produce about 5% Fe<sup>2+</sup> and 95% Fe<sup>3+</sup> very rapidly, and the mean life of the Fe<sup>3+</sup> in CoO at room temperature should be 1.4×10<sup>-7</sup> sec. Bhide and Shenoy<sup>3</sup> confirmed Wertheim's results, which were taken over the temperature range between 77 and 298°K, and they extended the experiment above room temperature

to about 1000°K. They also observed an increase in the intensity of Fe<sup>3+</sup> with increasing temperature, which was attributed to a monotonic increase in the relaxation time of Fe<sup>3+</sup> as the temperature increased.

We already reported<sup>4</sup> the results of our studies on CoO, which indicate no evidence for Auger aftereffects. Studies on many chemically simple materials such as CoCl<sub>2</sub> and CoI<sub>2</sub> also gave no evidence for Auger after-effects.<sup>7,8</sup> A form of cobaltous oxide which showed an Fe<sup>3+</sup> Mössbauer pattern without any Fe<sup>2+</sup> pattern was prepared, and our results indicated that the experiment of Wertheim resulted from two distinct forms of cobaltous oxide. Form I showed only Fe<sup>2+</sup> lines, while form II showed only Fe<sup>3+</sup> lines.

At almost the same time, and independently, Triftshäuser and Craig<sup>6</sup> reported no evidence for Auger aftereffects in CoO, using the time-delay technique, although they suggested, in contrast to our own proposal, that the observed Fe<sup>3+</sup> charge state could be interpreted in terms of a small excess of cation vacancies in CoO, associated with imperfect stoichiometry. This model, which was first suggested by Wertheim<sup>9</sup> and adopted by Triftshäuser and Craig,<sup>9,10</sup> will be subsequently referred to as the TC model. Their proposal of cation vacancies was mainly based on the electrical-

\* Work supported in part by the U.S. Atomic Energy Commission, under Contract No. (AT11-1) 1616.

† Based on a thesis research at Purdue University in partial fulfillment of the requirements for the degree of Doctor of Philosophy.

<sup>1</sup> G. K. Wertheim, *Phys. Rev.* **124**, 764 (1961).

<sup>2</sup> H. Pollak, *Phys. Status Solidi* **2**, 720 (1962).

<sup>3</sup> V. G. Bhide and G. K. Shenoy, *Phys. Rev.* **147**, 147 (1966).

<sup>4</sup> J. G. Mullen and H. N. Ok, *Phys. Rev. Letters* **17**, 287 (1966).

<sup>5</sup> C. J. Coston, R. Ingalls, and H. G. Drickamer, *Phys. Rev.* **145**, 409 (1966).

<sup>6</sup> W. Triftshäuser and P. P. Craig, *Phys. Rev. Letters* **16**, 1161 (1966).

<sup>7</sup> J. G. Mullen, *Phys. Rev.* **131**, 1410 (1963).

<sup>8</sup> D. W. Hafemeister, Ph.D. thesis, University of Illinois, 1964 (unpublished).

<sup>9</sup> B. Fisher and D. S. Tannhäuser, *J. Chem. Phys.* **44**, 1663 (1966).

<sup>10</sup> W. Triftshäuser and P. P. Craig, *Phys. Rev.* **162**, 274 (1967).

conductivity measurement on polycrystalline cobaltous oxide by Fisher and Tannhauser.<sup>9</sup> Using the x-ray diffraction patterns, which showed no diffraction rings not ascribable to CoO, Triftshäuser and Craig concluded that their sample was perfect, except for a possible small number of cation (+) vacancies. We already pointed out<sup>4</sup> that there may be difficulties in interpreting x-ray powder patterns for this material, and this point will be discussed fully in a later section of this paper, where we give in detail the results of our own x-ray studies. We also reported that the form II, CoO, converted irreversibly to the form I on heating in an inert atmosphere at elevated temperatures. This observation was not in accord with the claims of Triftshäuser and Craig, who asserted that the ratio of  $Fe^{2+}/Fe^{3+}$  was completely reversible on temperature cycling. Although variations in stoichiometries of CoO are possible, particularly for CoO(II), our results indicate that this is not the underlying reason why  $Fe^{2+}$  and  $Fe^{3+}$  [those corresponding to CoO(I) and CoO(II)] are observed in Mössbauer source experiments using cobaltous oxide.

The object of this paper is to present in detail the results of our recent studies on cobaltous oxide, and to show that these results can be explained neither by Auger aftereffects, nor by the TC model, but require a model based on the existence of two distinct forms of cobaltous oxide.

## II. PROPOSED MODEL FOR THE STRUCTURE OF COBALTOUS OXIDE

The essence of our model is that there are two distinct types of cobaltous oxide, referred to as CoO(I) and CoO(II). While it is possible to isolate these two materials, they are usually combined when the usual chemical recipes are followed. When they are combined, we will refer to the combination as CoO(I,II). Combined forms I and II have an interplay which depends on the concentration of II relative to I and on the temperature. In order to simplify the discussion, we shall enunciate our model, point by point, and in subsequent sections, we shall show how it is in harmony with a wide class of experimental findings, while other proposed models contradict our experimental results. We claim that cobaltous oxide has the structure enumerated in the following:

(1) There is a form of CoO, which we call CoO(I), having the NaCl structure with ideal stoichiometry and essentially perfect translational symmetry [Fig. 1(a)]. Its density, e.g., is 6.4 g/cm<sup>3</sup>, when measured by either x-ray analysis or a macroscopic density measurement. Mössbauer spectra of CoO(I) show only  $Fe^{2+}$  lines.

(2) There is a form of CoO, which we will call CoO(II), having the NaCl structure with half of its positive ion sites and half of its negative ion sites vacant [Fig. 1(b)]. While there is no long-range order

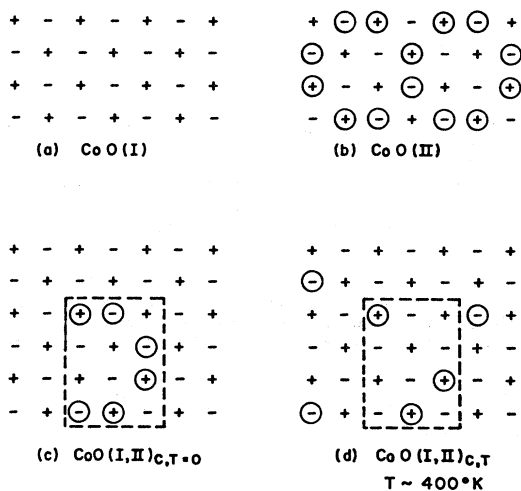


FIG. 1. Geometry of different forms as given in proposed model. (a) pure form (I) with no vacancies, (b) pure form (II) with 50% of its sites vacant. Any long-range order is less than 50 Å. Short-range order shown is arbitrary and not intended to show any actual known ordering. (c)  $CoO(I,II)_{C,T=0}$ , a simple mixture of CoO(I) and CoO(II) at 0°K. (d)  $CoO(I,II)_{C,T}$ , anion vacancies are partially dispersed for  $T > 200^\circ K$ .

to the vacancy arrangement, there may be and probably is short-range order (less than 50 Å). The density of this material is about 3.2 g/cm<sup>3</sup>, and its Mössbauer spectra show only  $Fe^{3+}$ .

(3) A mixture of CoO(I) and CoO(II) will be denoted generically as  $CoO(I,II)$ . At low temperatures (relative concentration of form II =  $C$ , temperature = 0),  $CoO(I,II)_{C,0}$  always consists of a simple mixture of CoO(I) and CoO(II) [Fig. 1(c)].

(4) At elevated temperatures ( $T > 200^\circ K$ ) there is an interplay between CoO(I) and CoO(II) such that the anion vacancies of the form II disperse into the form I lattice [Fig. 1(d)]. This interplay is what is responsible for the apparent increase in intensity of  $Fe^{3+}$  observed by Bhide and Shenoy,<sup>3</sup> and studied in more detail in the present work. Because the details of this interplay depend on the relative concentrations of form II compared with form I, we refer to it specifically as  $CoO(I,II)_{C,T}$ , where  $C$  denotes percentage concentration of the form II at  $T = 0^\circ K$ , and where  $T$  denotes the temperature of the measurement.

## III. MACROSCOPIC PROPERTIES

### A. Sample Preparation

We found two methods for preparing the unusual form of cobaltous oxide, CoO(II). This material could be formed either by heating  $CoCO_3$  in high vacuum or by reducing a higher oxide formed from a nitrate in a hydrogen atmosphere at low temperatures.

A radioactive solution of  $CoCl_2$  was mixed with slightly more than two molecular equivalents of

TABLE I. Stoichiometry of cobaltous oxide. Gravimetric determinations of  $X$  for basic forms of cobaltous oxide written as  $\text{CoO}_X$ .

Form Measurement	CoO(II) <sup>a</sup>	CoO(I, II)	CoO(I)
1	1.036(+0.010, -0.050)	0.99±0.02	1.02±0.03
2	1.043(+0.010, -0.050)	0.97±0.03	1.00±0.02 <sup>b</sup>
3	1.039(+0.010, -0.040)	0.99±0.05	
4		0.98±0.02	

<sup>a</sup> Although these values are slightly greater than 1, this was probably the results of argon adsorption as discussed in the text.

<sup>b</sup> A commercial-grade cobalt metal was used for this measurement.

$\text{NaHCO}_3$  to produce the following reaction in a  $\text{CO}_2$  atmosphere or an argon atmosphere at the boiling point of the mixture:



By removing  $\text{NaCl}$  by the water dilution method, we could get the radioactive  $\text{CoCO}_3$ , which was heated at  $300^\circ\text{C}$  in vacuum to give a very dark brown (almost black) material, which had the chemical composition  $\text{CoO}$ , and is the oxide form which we refer to by the label II. It was necessary to do the chemistry in a glove box filled with argon gas, because  $\text{CoO(II)}$  rapidly absorbs oxygen, a property which will be discussed later.

The hydrogen-reduction method was performed in the following way: A sample of cobaltous nitrate was heated at  $200^\circ\text{C}$  to produce a higher oxide of cobalt, which was reduced in a hydrogen atmosphere of about 200-mm-Hg pressure at about  $210^\circ\text{C}$  to give  $\text{CoO(II)}$ . This method had the limitation that it always gave a small amount of cobalt metal in the reduction process.

$\text{CoO(I)}$  can be prepared by heating cobalt metal in a carbon-dioxide atmosphere. After reducing  $\text{Co}_3\text{O}_4$  to  $\text{Co}$  metal at  $800\text{--}900^\circ\text{C}$  in a hydrogen atmosphere, we oxidized the metal in a carbon-dioxide atmosphere at  $1000^\circ\text{C}$  in a sealed quartz tube. The  $\text{CO}_2$  atmosphere was added after the hydrogen was evacuated. At the high temperatures used,  $\text{CO}_2$  partially disassociates, thereby permitting the oxidation of the cobalt metal. The specimen was quenched in a helium atmosphere from 1000 to  $0^\circ\text{C}$  in an ice bath and to  $77^\circ\text{K}$  in a liquid-nitrogen bath. The  $\text{CoO(I)}$  prepared by this method had a light brown color (almost yellow).

$\text{CoO(I,II)}$  can be prepared, as most people have done, by heating cobalt metal or cobaltous nitrate at  $1000^\circ\text{C}$  in air current and cooling it in an inert atmosphere like argon or nitrogen. The color of  $\text{CoO}$  prepared in this way was usually dark brown.

### B. Stoichiometry

The stoichiometries of  $\text{CoO(I)}$ ,  $\text{CoO(II)}$ , and  $\text{CoO(I,II)}$  were determined by a combination of gravimetric, x-ray, and Mössbauer measurements. For

the preparation of these oxides, 99.999%  $\text{Co}$  and 99.999%  $\text{HNO}_3$  were used, and weights were determined by using a Mettler semimicro balance. In order to determine the weight loss due to evaporation, we started from cobalt metal and returned to cobalt metal after measuring the weights of  $\text{CoO}$ . The measured weight losses were within 0.3% of the sample weight. X-ray diffraction patterns were taken to show that these materials had the correct crystal structures (see Sec. V for detailed discussion). The form of each specimen was assessed by a Mössbauer measurement. Several measurements showed that all of  $\text{CoO(I)}$ ,  $\text{CoO(II)}$ , and  $\text{CoO(I,II)}$  have the chemical composition  $\text{CoO}_{1.00\pm 0.05}$  shown in Table I. Special care was taken in weighing  $\text{CoO(II)}$ , because  $\text{CoO(II)}$  absorbs oxygen very rapidly in air. An aluminum capsule with airtight rubber seal was used. While the values of  $X$  for  $\text{CoO(II)}$  appear slightly greater than one, we believe that this is not significant, because the highly vacated form II gave visible evidence for argon adsorption on the surface.

### C. Density

Since  $\text{CoO(I)}$  has a perfect  $\text{NaCl}$  structure with a lattice parameter of  $a_0 = 4.26 \text{ \AA}$  at  $20^\circ\text{C}$ , its density should be  $6.4 \text{ g/cm}^3$ . In contrast to earlier measurements,<sup>11</sup> our measurement showed that the density of  $\text{CoO(I)}$  was  $6.4 \pm 0.1 \text{ g/cm}^3$ , in excellent accord with the predicted value based on the measured lattice parameter.

On the other hand,  $\text{CoO(II)}$  was found to have a density of about  $3.2 \text{ g/cm}^3$ , nearly half of the value found for  $\text{CoO(I)}$ . In Table II, we list several measured values of the density of  $\text{CoO(II)}$ . Although the inherent difficulties in the measurement are such that a precise value of the density was not possible, we take the best value to be  $\rho = 3.2 (+1.0, -0.0) \text{ g/cm}^3$ , where the lower limit rather than the average value has been chosen on the grounds that the more likely value is the one obtained from low-temperature preparation, where

TABLE II. Densities of  $\text{CoO}$ .

Material	Measured density (uncorrected) ( $\text{g/cm}^3$ )	Corrected density ( $\text{g/cm}^3$ )	Temperature of preparation ( $^\circ\text{C}$ )
	5.7	$3.4 \pm 0.5$	210
	3.7	$3.6 \pm 0.5$	210
	4.7	$3.3 \pm 0.5$	210
$\text{CoO(II)}$	5.6	$4.5 (+0.5, -1.5)$	300
	5.1	$4.8 (+0.5, -1.5)$	300
	5.1	$4.8 (+0.5, -1.5)$	300
$\text{CoO(I)}$	$6.38 \pm 0.10$	$6.38 \pm 0.10$	1000

<sup>11</sup> J. W. Mellor, *A Comprehensive Treatise on Inorganic and Theoretical Chemistry* (Longmans Green and Co., Inc., New York, 1935), Vol. XIV.

the transformation of form II to I was negligible (see Sec. III E).

The technique used for the density measurements was the standard volume-gravimetric approach with carbon tetrachloride as a nonreactive liquid in which the various materials were immersed for volume determination by weighing with a Mettler semimicro balance. For materials which could be prepared in a completely pure form, such as NaCl, Co, etc., the measured densities were within about 2% of the expected values. CoO(II) presented particular problems, however, because the large quantity required for the density measurement ( $\sim 3$ g) precluded the possibility of synthesizing the material without some admixture of CoO(I). This was basically because large samples required longer anneals which resulted in the transformation  $\text{CoO(II)} \rightarrow \text{CoO(I)}$ , a phenomenon which was studied in detail and will be described later. Because of this contamination, the data given in Table II show the raw values for densities of the actual samples, and values "corrected" for CoO(I) contamination. This correction factor was based on Mössbauer measurements on the same material as used in the density measurements. The errors inherent in the estimate of the correction factor are such that all values are consistent with  $\rho_{\text{II}} = 3.2 \text{ g/cm}^3$ , but no value of  $\rho_{\text{II}}$  can be greater than  $4.8 \text{ g/cm}^3$ .

Although all macroscopic measurements such as density have their limitations and can be misleading if not correlated with other experimental evidence, the

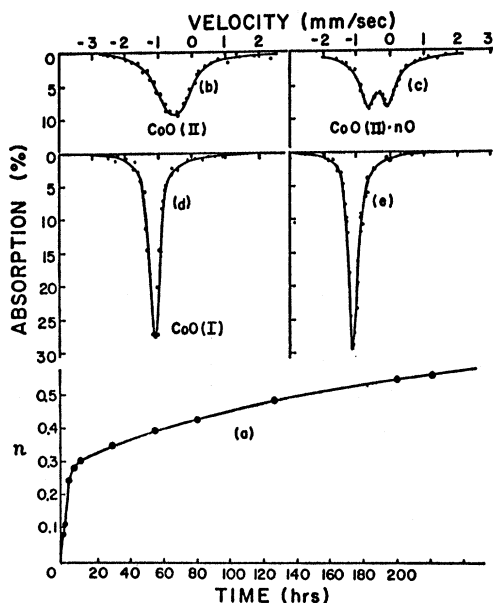


FIG. 2. Oxidation properties of CoO(I) and CoO(II). (a) oxygen absorption of CoO(II) as a function of time, as determined by increasing weight. For  $\text{CoO(II)} \cdot n\text{O}$ ,  $n$  is shown as the ordinate. (b) and (c) Mössbauer spectra at  $26^\circ\text{C}$  of CoO(II) before and after exposure to oxygen. (d) and (e) Mössbauer spectra at  $26^\circ\text{C}$  of CoO(I) before and after exposure to air for 2 months.

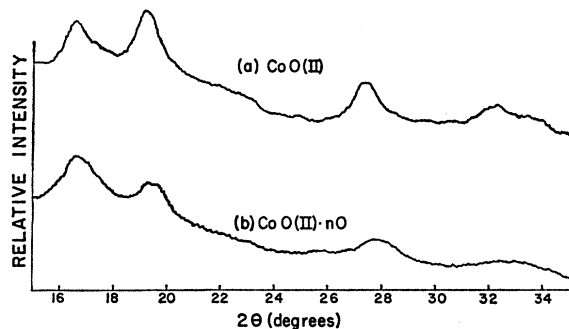


FIG. 3. X-ray diffraction patterns of CoO(II) before (a) and after (b) exposure to air. Mo  $K\alpha$  was used for taking the powder patterns.

following additional precautions were taken in an attempt to make the measurement as meaningful as possible.

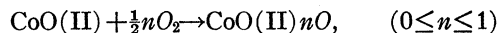
(1) Powder specimens, which were submerged in Grade "A" volumetric flasks, were pumped with a forevacuum system to eliminate gas bubbles.

(2) It was experimentally verified that  $\text{CCl}_4$  did not react with cobaltous oxide by observing the Mössbauer spectrum of a submerged sample.

(3) The experimental determination was repeated several times to check for reproducibility. The results in Table II indicate satisfactory reproducibility in the light of the experimental difficulties.

#### D. Oxidation Properties

One of the most noteworthy properties of CoO(II), which had been observed<sup>12,13</sup> prior to our work, is the rapid absorption of oxygen by the porous CoO(II) lattice. We observed the effect in a direct gravimetric measurement of the weight as a function of the time of exposure to air, and the effect was further verified by observing the transformation of the CoO(II) Mössbauer pattern after exposure to air. The time dependence of the reaction



as determined by weights, is shown in Fig. 2.

The Mössbauer spectra before and after oxygen absorption are shown in Fig. 2. For comparison, we show how vacancy-free CoO(I) is completely unaffected after two months' exposure to air. The Mössbauer spectrum of oxygen-saturated CoO(II) has a double line different from that of CoO(II), while the x-ray powder pattern of oxygen-saturated CoO(II) shown in Fig. 3 is in fact nearly the same as that of CoO(II). The invariance of the x-ray pattern under oxygen absorption was already observed by chemists.<sup>12</sup> It

<sup>12</sup> N. V. Sidgwick, *Chemical Elements and Their Compounds* (Clarendon Press, Oxford, England, 1952), Vol. II.

<sup>13</sup> M. le Blanc and J. E. Möbius, *Z. Physik. Chem. (Leipzig)* **142**, 151 (1929).

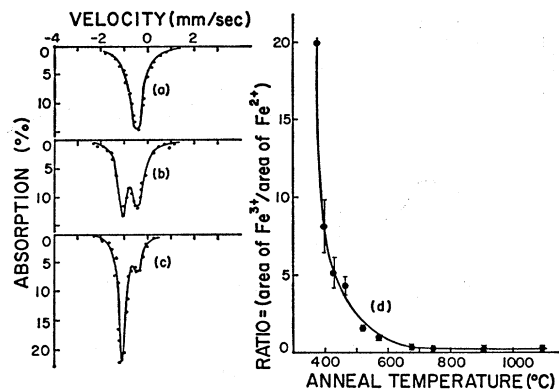


FIG. 4. Conversion of CoO(II) to CoO(I) in an argon atmosphere. Three examples of Mössbauer spectra taken at room temperature after the sample was heated for 20 min in an argon atmosphere at temperature (a) 24°C, (b) 523°C, and (c) 750°C; (d) the ratio of area of Fe<sup>2+</sup> to that of Fe<sup>3+</sup> at room temperature is shown, after heating the sample at each temperature indicated for 20 min successively.

suggests that the oxygen which diffuses into the CoO(II) lattice fills the anion vacancies of this porous lattice. This additional interstitial oxygen in CoO(II) destroys the internal magnetic field at the Fe<sup>57</sup> nucleus but, as expected, has slight effect on the x-ray powder pattern. A detailed discussion of our x-ray studies on cobaltous oxide will be given later.

### E. Thermal Hysteresis

It would be reasonable to expect a highly vacated structure such as CoO(II) to be a metastable state, which would transform to stable CoO(I) when sufficient thermal energy is supplied. In fact, CoO(II) transformed noticeably to CoO(I) above about 300°C with a transformation rate that increased with temperature. The ratio of Fe<sup>2+</sup> to Fe<sup>3+</sup> shown in Fig. 4 was determined from the Mössbauer spectra at 24°C after the sample was heated at each temperature for 20 min in an argon atmosphere.

The conversion of CoO(II)→CoO(I) on heating in argon was never completed up to about 1000°C for the time period of several hours, and generally left a small number of Schottky defects, giving CoO(I,II). As we will show in the subsequent discussion, this small number of Schottky defects is not the true equilibrium concentration, but is a nonequilibrium thermodynamic distribution, even though reversible Mössbauer spectra are observed under temperature cycling below 1000°K. Our results indicate that the time required to achieve true thermodynamic equilibrium at these temperatures is large compared with the experimental times. These temperature-dependent Mössbauer results, which give the false appearance of representing a reversible process, were observed previously<sup>3,6</sup> and agree in essence with our own findings.

### F. Pressure and Quenching Experiments

When CoO(I,II) was placed in a mechanical press and an external pressure of approximately 10<sup>4</sup> atm was applied to the sample at room temperature (24°C), it was hoped that CoO(II) might be transformed to CoO(I). Figures 5(a) and 5(b) show the Mössbauer patterns before and after the application of pressure. While the lines broaden, there is no clear-cut conversion of II to I, indicating that a pressure of 10<sup>4</sup> atm is insufficient to effect the transformation at 24°C. We did not have the facilities to test whether the transformation could be achieved at higher pressure even at room temperature. A variation of the pressure experiment was done by quenching a specimen of CoO(I,II) from 600 to 0°C and then to 77°K. This experiment was performed in a copper tube filled with an inert atmosphere to ensure rapid cooling in a chemically inactive environment. Although such an experiment lacks sufficient control to permit an accurate assessment of the pressures and stresses placed on the powder specimen, they were found to be large enough to cause the porous form II to transform to the "vacancy-free" pure form I. The Mössbauer patterns giving these results are also shown in Figs. 5(c) and 5(d), where a sizable fraction of the Fe<sup>3+</sup> room-temperature line is seen to convert to the Fe<sup>2+</sup> line.

## IV. MOSSBAUER SPECTRA

### A. Method of Mössbauer Spectrometry

Our method of velocity spectrometry has been described earlier.<sup>7</sup> The Mössbauer resonances were observed using a mechanical velocity spectrometer, which produced a crank motion at the absorber. While the absorber executed a continuous reciprocating crank motion in time,  $\gamma$  rays from Fe<sup>57</sup> nuclei were analyzed with a gas-filled proportional counter, a preamplifier, and a single-channel analyzer. The pulses from the

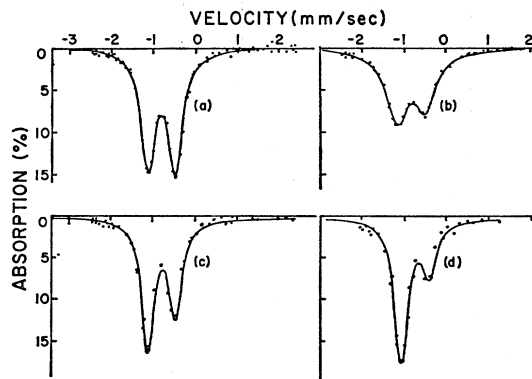


FIG. 5. Effects of pressure and quenching on the conversion of CoO(II) to CoO(I). Mössbauer spectra (a) before applying pressure, (b) after applying pressure, (c) before quenching, and (d) after quenching.

14.4-keV  $\gamma$  rays were then sent into a 400-channel RIDL multichannel analyzer, which was operated as a multichannel scaler, with the channel address being advanced linearly in time, via an independent oscillator. The analyzer system was reset synchronously with the reciprocating motion by a pulse generated from a photodiode.

Narrow unsplit sodium-ferrocyanide absorbers of various effective thicknesses in  $\text{Fe}^{57}$  (0.5, 0.75, and 1.0  $\text{mg}/\text{cm}^2$ ) made by New England Nuclear Corporation were used in this work. Throughout this work, the absorbers were kept at room temperature, while the temperatures of the sources were varied.

### B. Mössbauer Spectra

In Fig. 6, Mössbauer spectra of CoO(I) are shown as a function of temperature. Above  $288^\circ\text{K}$  the spectra are single lines, but below  $288^\circ\text{K}$  they split because of a magnetic hyperfine interaction.

Bizette<sup>14</sup> and LaBlanchetais<sup>15</sup> have reported that cobaltous oxide is an antiferromagnetic substance with a Néel temperature of about  $291^\circ\text{K}$ . Therefore, the single lines observed above  $288^\circ\text{K}$  represent paramagnetic states above the Néel temperature, and the hyperfine patterns below  $288^\circ\text{K}$  correspond to the anti-

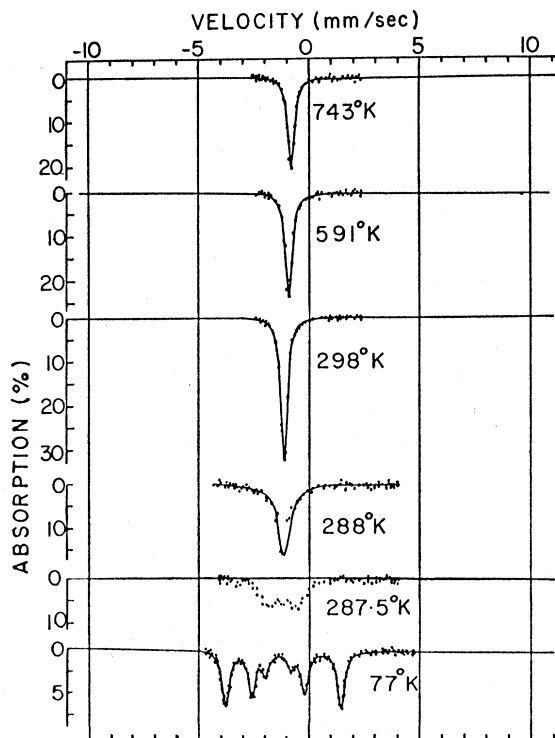


FIG. 6. Mössbauer spectra for CoO(I) as a function of temperature. A 0.75- $\text{mg}/\text{cm}^2$   $\text{Na}_4\text{Fe}(\text{CN})_6 \cdot 10\text{H}_2\text{O}$  absorber was used.

<sup>14</sup> H. Bizette, *J. Phys. Radium* **12**, 161 (1951).

<sup>15</sup> C. H. LaBlanchetais, *J. Phys. Radium* **12**, 765 (1951).

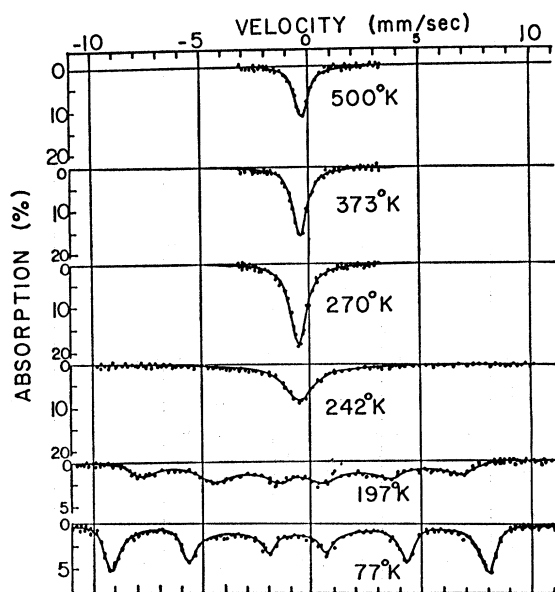


FIG. 7. Mössbauer spectra for CoO(II) as a function of temperature. A 1.0- $\text{mg}/\text{cm}^2$   $\text{Na}_4\text{Fe}(\text{CN})_6 \cdot 10\text{H}_2\text{O}$  absorber was used.

ferromagnetic state. The apparent Néel temperature in our experiment is then  $288^\circ\text{K}$ ,  $3^\circ$  less than that reported by Bizette and LaBlanchetais. This  $3^\circ$  discrepancy is outside of our experimental errors and probably reflects the limited accuracy of the earlier techniques.<sup>14,15</sup>

The isomer shift of CoO(I) at  $26^\circ\text{C}$  relative to  $\text{Na}_4\text{Fe}(\text{CN})_6 \cdot 10\text{H}_2\text{O}$  absorbers is  $-1.12$   $\text{mm}/\text{sec}$ . From a comparison with the systematics of the isomer shift<sup>16,17</sup> the Mössbauer lines from CoO(I) correspond to the divalent compounds. The magnetic hyperfine field at  $0^\circ\text{K}$ , about 120 kG, also corresponds to the divalent charge state.<sup>17</sup> (The full discussion on the magnetic hyperfine and quadrupole interactions will be given in detail in the following paper.<sup>18</sup>) The divalent charge state of  $\text{Fe}^{57}$  in CoO(I) established by the isomer shifts and the magnitude of the magnetic hyperfine field is consistent with our model that CoO(I) has a perfect NaCl structure with essentially no vacancies.

Mössbauer spectra of CoO(II) over a wide range of temperatures are shown in Fig. 7. (For more patterns at other temperatures, see the following paper.<sup>18</sup>) Above  $270^\circ\text{K}$  the spectra are single lines, but below  $270^\circ\text{K}$  they split into the six-finger patterns, in addition to a very broad line with unresolvable structure, whose linewidth becomes broader with decreasing temperature, and whose depth approaches zero at  $77^\circ\text{K}$ . This differed from the magnetic hyperfine patterns of CoO(I), which showed a well-defined transition from a six-finger pattern to a single line at  $288^\circ\text{K}$ .

<sup>16</sup> S. DeBeneditti, G. Lang, and R. Ingalls, *Phys. Rev. Letters* **6**, 60 (1961).

<sup>17</sup> K. Ono and A. Ito, *J. Phys. Soc. Japan* **19**, 899 (1964).

<sup>18</sup> H. N. Ok and J. G. Mullen, following paper, *Phys. Rev.* **168**, 563 (1968).

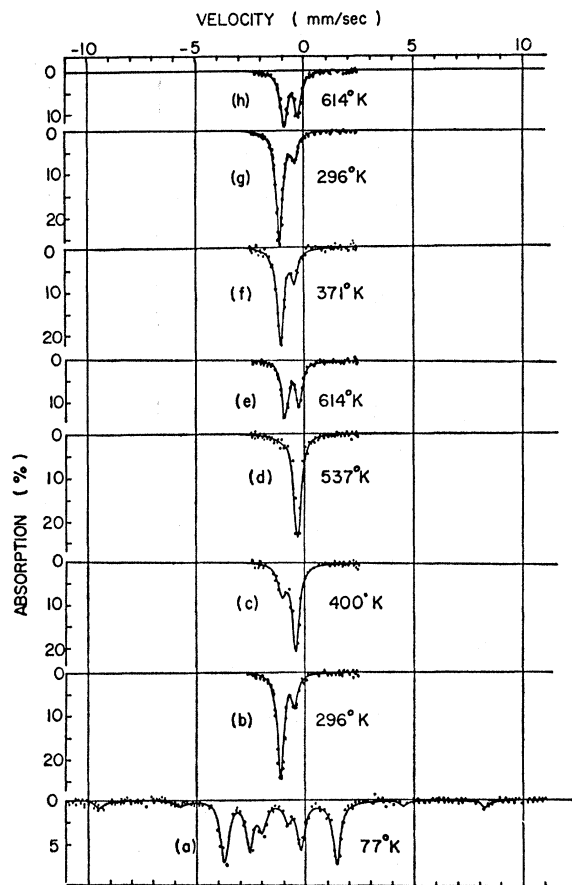


FIG. 8. Mössbauer spectra of CoO(I, II) as a function of temperature.

As the temperature approached the transition temperature of about 270°K, the broad unresolved line in the Mössbauer spectra of CoO(II) grew and gradually became a single line with the disappearance of the six-finger pattern (Fig. 7). Because the broad unresolved line was superimposed on the observed hyperfine pattern, it was difficult to measure the Néel temperature accurately. A Néel temperature of about 270°K was determined from the maximum intensity value of the single line and should be accurate to within  $\pm 10^\circ\text{K}$ . From the results of x-ray diffraction (see Sec. V) it is shown that there is no long-range ordering greater than 50 Å for the pure CoO(II) structure, even though short-range ordering can still exist. One way of explaining the broad unresolved line is to assume that a fraction of the cobaltous ions in CoO(II) are in disturbed environments from those which show the resolvable hyperfine pattern. This could result from domain boundaries in form II. The observed x-ray pattern shows that these domains could not be appreciably larger than 50 Å. Their influence could also be the reason why the resolvable part of the hyperfine pattern showed a substantially broader linewidth than was

observed for CoO(I). The possibility of domains in CoO(II) was not studied in sufficient detail to establish its validity, although no evidence was found which contradicted this hypothesis.

The isomer shift of CoO(II) at 26°C relative to a sodium-ferrocyanide absorber is  $-0.45$  mm/sec. This value is a characteristic value for  $\text{Fe}^{3+}$ , as shown in many ferric compounds.<sup>16</sup> The low-temperature magnetic hyperfine field for  $\text{Fe}^{57}$  in CoO(II) was found to be 553 kG and is characteristic<sup>19,20</sup> of compounds containing  $\text{Fe}^{3+}$ . The trivalent charge state of  $\text{Fe}^{57}$  in CoO(II) can be understood within the framework of our model by assuming that the surrounding negative-ion vacancy traps one of the electrons from the iron ion, making a defect pair of  $\text{Fe}^{3+}$  associated with an electron trapped at an anion vacancy.

In Fig. 8, Mössbauer spectra of  $\text{CoO(I,II)}_{c,T}$  consist of two kinds of lines, which can be easily identified with  $\text{Fe}^{2+}$  and  $\text{Fe}^{3+}$ , respectively, when these are compared with the spectra of CoO(I) and CoO(II) shown in Figs. 6 and 7. These mixed spectra of  $\text{Fe}^{2+}$  and  $\text{Fe}^{3+}$  in CoO(I,II) were first observed by Wertheim<sup>1</sup> and lately by many others.<sup>3-6</sup> Various interpretations for these results have been given, which we already mentioned in Sec. I, and will discuss in detail in Sec. VI. While the temperature dependence of the magnetic hyperfine field of  $\text{Fe}^{2+}$  in CoO(I,II) is the same as that for pure CoO(I) over the full range of temperatures, the magnetic hyperfine field of the  $\text{Fe}^{3+}$  component of CoO(I,II) is very similar at low temperatures to that of the pure CoO(II), having a slightly higher Néel temperature than  $\text{Fe}^{3+}$  in pure CoO(II), and in fact the same transition temperature as that of CoO(I). This phenomena can be easily explained by our model, which postulates a gradual dispersion of anion vacancies into the CoO(I) structure as the temperature is raised above 200°K. These dispersed anion vacancies cause any surrounding  $\text{Co}^{57}$  ions to transform to  $\text{Fe}^{3+}$  after radioactive decay, but the Néel temperature will now correspond to that of CoO(I) instead of CoO(II). Strong additional evidence for this dispersion of negative-ion vacancies will be discussed at the end of this section.

In addition to source experiments, Mössbauer absorbers of CoO doped with enriched  $\text{Fe}^{57}$  were studied. Two absorbers were made, one starting from a chloride and the other starting from a nitrate.

The first absorber was prepared by reducing  $\text{CoCl}_2$  doped with  $\text{FeCl}_2$  to metallic  $\text{Co}:\text{Fe}^{57}$  in a hydrogen atmosphere above 600°C, and then heating the resulting  $\text{Co}:\text{Fe}^{57}$  in a carbon-dioxide atmosphere at 950°C for 5 h. X-ray diffraction patterns of this absorber were exactly the same as those generally found for CoO(I). For this absorber experiment  $\text{Co}^{57}$  in Cu was used as a

<sup>19</sup> O. C. Kistner and A. W. Sunyar, Phys. Rev. Letters **4**, 412 (1960).

<sup>20</sup> G. K. Wertheim, J. Appl. Phys. Suppl. **32**, 110 (1961).

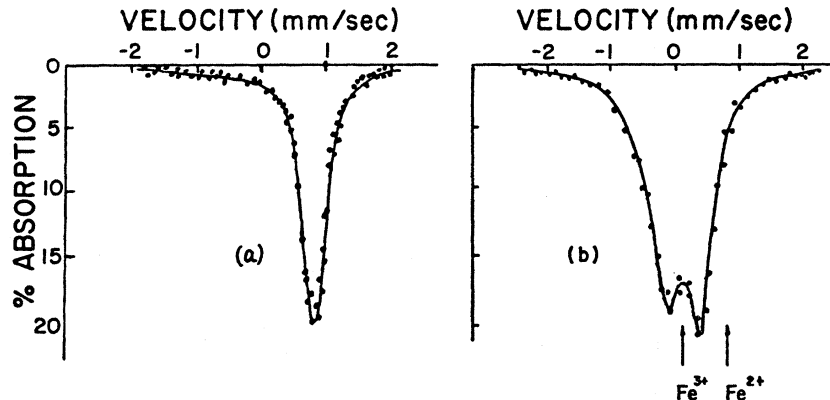


FIG. 9. Mössbauer spectra at 26°C for the  $Fe^{57}$ -doped cobaltous oxide absorbers.  $Co^{57}$  in Cu was used as the source. (a) prepared from a chloride, (b) prepared from a nitrate. Two arrows show the line positions corresponding to  $Fe^{2+}$  and  $Fe^{3+}$  in CoO(I, II).

Mössbauer source. Since the isomer shift of  $Co^{57}$  in Cu relative to a sodium-ferrocyanide absorber is  $-0.27$  mm/sec, an isomer shift  $0.87$  mm/sec for this absorber [Fig. 9(a)] using a  $Co^{57}$  in Cu source is equivalent to an isomer shift of  $-1.14$  mm/sec for  $Fe^{2+}$  in CoO relative to a sodium-ferrocyanide absorber. Because this is the identical isomer shift found in the source experiments for  $Fe^{2+}$  in CoO(I), we conclude that  $Fe^{2+}$  in a CoO(I) absorber is identical to  $Fe^{2+}$  resulting from the decay of  $Co^{57}$  in CoO(I).

The second absorber was prepared by heating a nitrate at 990°C in an oxygen atmosphere for 1 h and in a nitrogen atmosphere for 3 h. X-ray diffraction patterns of this absorber were again of the same type as a cobaltous oxide. The Mössbauer spectra for this absorber, however, showed two lines which corresponded to  $Co^{57}$ -doped  $Co_3O_4$  [Fig. 9(b)].

Triftshäuser and Craig<sup>6,10</sup> also prepared two absorbers, one starting from a chloride and the other starting from a nitrate. Although their resonances showed a small percentage effect because natural iron was used, they claimed that their observed spectra were essentially identical to those obtained using the CoO source. We made two more absorbers, in addition to the above-mentioned ones, using enriched  $Fe^{57}$  instead of natural Fe, and following the identical recipes as those of Triftshäuser and Craig<sup>10</sup>; but we obtained the same spectra, as shown in Fig. 9(b). The only technique which was found to permit the substitutional implantation of  $Fe^{3+}$  in CoO(II) was that resulting from the radioactive decay from a cobalt parent. It was therefore only possible to observe this resonance in source experiments.

### C. Temperature Dependence of Recoil-Free Fraction

Mössbauer recoil-free fraction, or  $f$  factor, is proportional to the area under the Mössbauer absorption pattern, and can be expected to decrease as source temperature is increased. This is true for both pure CoO(I) and pure CoO(II) [Figs. 10(a) and 10(e)]. On the other hand, the general decreasing tendency of

$f(T)$  does not hold for a material such as CoO(I,II)<sub>c,r</sub>, because of the dispersion of anion vacancies at higher temperatures. This dispersion substantially increases the probability that any given  $Co^{57}$  ion will have an adjoining negative-ion vacancy, which results in the formation of  $Fe^{3+}$  following the radioactive decay of  $Co^{57}$ . This interplay between CoO(I) and CoO(II) at higher temperatures can, and in fact does, cause the area under the  $Fe^{3+}$  absorption curve to increase as the temperature is raised.

In the simple Debye model of a monatomic lattice the recoil-free fraction can be written as

$$f \simeq \exp\left[-\frac{3}{2}\left(\frac{R}{k\theta_M}\right)\left(1 + \left(\frac{2\pi^2}{3\theta_M^2}\right)T^2\right)\right], \quad (T < \theta_M)$$

where  $R$  is the recoil energy,  $\theta_M$  is the Mössbauer characteristic temperature, and  $k$  is Boltzmann's constant. Since the area under the Mössbauer absorption spectrum is proportional to  $f$ , the natural logarithm of the area can be written as

$$\ln A = a + b(T)T^2,$$

where  $a$  is a constant and

$$b(T) \simeq -R\pi^2/k\theta_M^3, \quad \text{for } T < \theta_M.$$

Even though these formulas only apply to a monatomic lattice with a Debye frequency spectrum, they are commonly used with more complex lattices, where it is understood that the effective  $\theta_M$  determined may have little relation to the Debye temperature obtained from specific-heat measurements. In Fig. 10,  $\ln A$  versus  $T^2$  for  $Fe^{2+}$  and  $Fe^{3+}$  in cobaltous oxide is shown with the total area under the entire Mössbauer spectrum adjusted to the same value in the very low-temperature limit, i.e.,  $T \ll \theta_M$ . Figure 10(a) represents pure CoO(I), which gives an effective Mössbauer characteristic temperature of 510°K from the above equation. CoO(II) has an effective characteristic temperature of only 320°K, however, which is much lower than that of CoO(I).

This much lower value of  $\theta_M$  for CoO(II) is in complete accord with our model for form II. The removal of



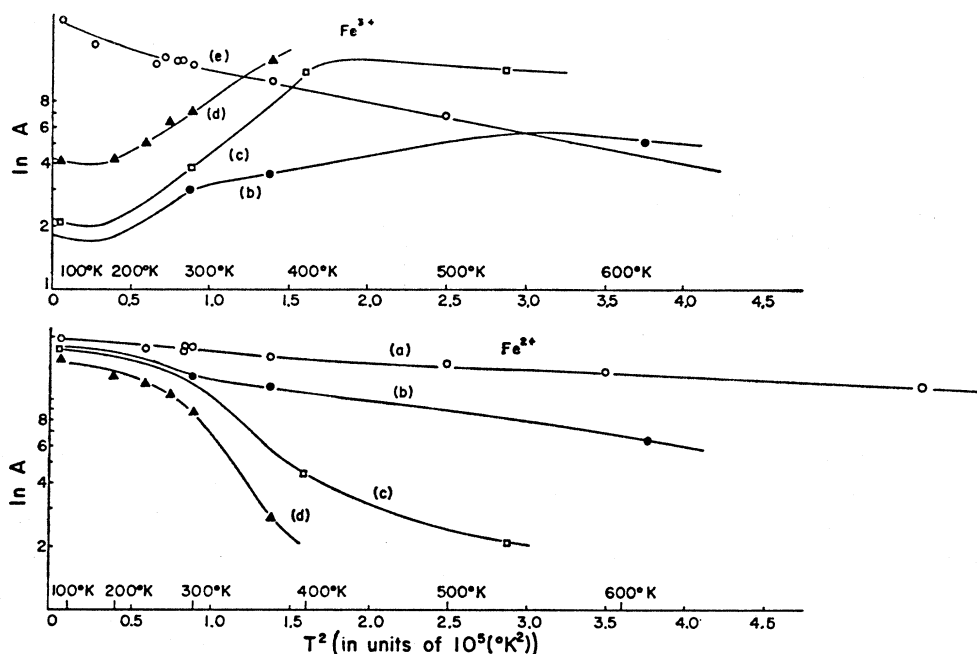


FIG. 10. Temperature dependence of  $\ln A$ , which is proportional to  $\ln f$  for  $\text{Fe}^{2+}$  and  $\text{Fe}^{3+}$  in cobaltous oxide. (a) pure  $\text{CoO(I)}$ , (b)  $\text{CoO(I, II)}_{9\%T}$ , (c)  $\text{CoO(I, II)}_{11\%T}$ , (d)  $\text{CoO(I, II)}_{21\%T}$ , (e) pure  $\text{CoO(II)}$ , where % represents  $\text{CoO(II)}$  concentration at  $0^\circ\text{K}$ .

half of the lattice ions means that a cobalt ion in form II has only half as many covalent bonds as a cobalt ion in form I, and so form-II nuclei are expected to be less tightly bound. The large difference in effective Mössbauer characteristic temperature is in the right direction and of the correct magnitude required by our model.

In Figs. 10(b), 10(c), and 10(d), the intermediate cases between the above two limits are shown, with the relative percentages of areas under the  $\text{Fe}^{3+}$  absorption spectra compared with the total absorption areas at  $0^\circ\text{K}$ . It might at first seem surprising that the areas of  $\text{Fe}^{3+}$  increase with increasing temperature, while those of  $\text{Fe}^{2+}$  decrease more rapidly than that of pure  $\text{CoO(I)}$ . This tendency for the  $\text{Fe}^{3+}$  areas to increase with increasing temperature was also observed by Bhide and Shenoy,<sup>3</sup> who attributed this increasing intensity of  $\text{Fe}^{3+}$  to a reversible increase in the relaxation time of  $\text{Fe}^{3+}$  with increasing temperature. Later, Triftshäuser and Craig<sup>6,10</sup> interpreted this increase in  $\text{Fe}^{3+}$  as a reversible oxidation, which caused an increase of cation vacancies. We found an irreversible process, however, which is in contradiction to both the reversible increase in the electronic relaxation time model and the reversible oxidation model. In Fig. 8, Mössbauer spectra for  $\text{CoO(I,II)}$  are arranged in the order of an actual thermal cycle, starting from (a) and ending with (h). The intensity of the  $\text{Fe}^{3+}$  Mössbauer line became larger as the temperature increased from  $296^\circ\text{K}$ , and practically none of the  $\text{Fe}^{2+}$  line remained at  $537^\circ\text{K}$ . When the temperature reached  $614^\circ\text{K}$ , however, a large fraction of the cobalt environments producing  $\text{Fe}^{3+}$  converted irreversibly to  $\text{Fe}^{2+}$  environments. After this irreversible

conversion, the Mössbauer spectra were reversible under temperature cycling for a time period comparable to the experimental times. Our observation that  $\text{Fe}^{3+}$  at  $614^\circ\text{K}$  converted to  $\text{Fe}^{2+}$ , as shown in Fig. 8, is not only in contradiction to the idea of a reversible increase of electronic relaxation time for  $\text{Fe}^{3+}$ , proposed by Bhide and Shenoy, but also is not in harmony with the assertion of Triftshäuser and Craig<sup>6,11</sup> that oxidation increases with increasing temperature. According to our model, however,  $\text{CoO(I,II)}$  consists of  $\text{CoO(I)}$  and  $\text{CoO(II)}$  at  $0^\circ\text{K}$ , with  $\text{CoO(II)}$  consisting of clusters formed by the precipitation of Schottky defects. When the temperature is raised sufficiently ( $\sim 200^\circ\text{K}$ ), our results indicate that the anion vacancies begin to move out of the precipitated vacancy clusters of  $\text{CoO(II)}$ . Dispersing the anion vacancies increases the probability of forming  $\text{Fe}^{3+}$ , because any given  $\text{Co}^{37}$  ion will now have approximately a fivefold greater chance of adjoining an anion vacancy. This dispersion of anion vacancies is supported by  $\text{CoO(II)}$  at room temperature described earlier, which demonstrates the mobility of the anion vacancies at these temperatures. As temperature increases, the fraction of disassociated anion vacancies increases, thereby enhancing the  $\text{Fe}^{3+}$  Mössbauer pattern while decreasing the  $\text{Fe}^{2+}$  component, until the temperature reaches a critical temperature of about  $600^\circ\text{K}$ , at which point large clusters of  $\text{CoO(II)}$  irreversibly collapse to give  $\text{CoO(I)}$ , leaving only small clusters of  $\text{CoO(II)}$  behind. The irreversible conversion of large clusters of  $\text{CoO(II)}$  to  $\text{CoO(I)}$  was demonstrated for pure  $\text{CoO(II)}$  in Sec. III E, but the small clusters of  $\text{CoO(II)}$

left behind apparently could not be eliminated by heating up to 1000°C, for typical experimental time periods. Even though these small clusters of CoO(II) give a reversible Mössbauer spectrum under temperature cycling up to 1000°K, they do not represent a true thermodynamic equilibrium concentration, because the Mössbauer spectrum of the pure CoO(I) is also reversible under temperature cycling, as shown in Fig. 10(a). The true thermodynamic equilibrium concentration was not determined, because of the size of the relaxation times at the temperatures accessible in our experiment. It is speculated, however, that pure CoO(I) is very close to that of the true thermodynamic equilibrium concentration, of defects, because alkali halides have very small equilibrium concentration of Schottky defects at comparable temperatures. The apparent invariance of Schottky-defect concentration below 1000°C is explained by a long relaxation time for reaching thermodynamic equilibrium, and the above-mentioned reversibility of Mössbauer spectra under temperature cycling also can be understood on this basis. Our results indicate that progressively more anion vacancies are disassociated from cation vacancies with increasing temperatures and are dispersed into the CoO(I) structure, thereby increasing the Fe<sup>3+</sup> Mössbauer line intensity, and when the temperature decreases, the dispersed anion vacancies are attracted toward the immobile cation vacancies by Coulomb attraction, giving the apparently reversible Mössbauer spectra.

We shall explain the thermal cycle drawn in Fig. 8, using our model and Fig. 10. We shall start with the 296°K points along curves 10(c). As the temperature increases, the Fe<sup>2+</sup> and Fe<sup>3+</sup> spectra follow curves 10(c) until the critical temperature of about 600°K is reached, and then an irreversible transformation occurs which corresponds to a vertical transformation from Figs. 10(c) to 10(b). Temperature cycling below 1000°K does not cause any further transformation, although, as we stated earlier, this does not necessarily represent the true thermodynamic equilibrium at these temperatures. It should be noted that the Fe<sup>3+</sup> part of the curve 10(c) at higher temperatures is even greater than that of pure CoO(II), as is shown in Fig. 10(e), and is comparable with 10(a) for pure CoO(I). This phenomenon strongly supports our model, because the Fe<sup>3+</sup> Mössbauer line of CoO(I,II) at higher temperatures results from the disassociated anion vacancies diffused into CoO(I), and consequently would be expected to approximately follow the recoil-free fraction curve of CoO(I) instead of pure CoO(II). A similar phenomenon is found with respect to the Néel temperature. For  $T_N$  is 288°K for both Fe<sup>2+</sup> and Fe<sup>3+</sup> in CoO(I,II)<sub>C,T</sub>, having only small clusters of form II ( $C < 20\%$ ), even though the Néel temperature of pure CoO(II) is slightly lower ( $\sim 18^\circ\text{K}$ ) than that of pure CoO(I). This effect is also explained by our model, i.e., the Fe<sup>3+</sup> in CoO(I,II)<sub>C,T,300°K</sub> is associated with

TABLE III. Relative line intensities of x-ray patterns of cobaltous oxide.

$2\theta$	Theoretical values		Experimental values	
	CoO(I) and CoO(II)	25% cation vacancies	CoO(I)	CoO(II)
16.6	71	49	70	73
19.2	100	100	100	100
27.3	64	63	63	66
32.1	35	26	32	38
33.6	21	20	22	18
39	9	9	9	7
42.7	14	11	14	10
43.8	24	23	22	18

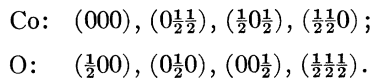
anion vacancies dispersed into CoO(I), and therefore may be expected to have the Neel temperature of the host material, CoO(I).

### V. X-RAY PATTERNS

The x-ray diffraction technique has been used for the determination of crystal structures for many years. For a perfect crystal structure with complete translational symmetry the line positions and relative intensities of the diffraction peaks are unique.<sup>21,22</sup> This is not necessarily true for a structure having many Schottky defects like CoO(II), which gives the same line positions and relative intensities as are found for perfect CoO(I).

The experimental x-ray patterns of CoO(I) and CoO(II) are shown in Fig. 11, which were obtained by using a powder x-ray diffractometer, made by North American Philips Co., along with a Geiger counter and a chart drive. From Fig. 11 the experimental line positions and relative intensities for CoO(I) and CoO(II) were calculated and listed in columns 1, 4, and 5 of Table III. It is clearly seen that the line positions and relative intensities are the same for both CoO(I) and CoO(II), even though the linewidths are much broader for form II than for form I.

CoO(I) has the perfect NaCl structure, having four cobalt atoms and four oxygen atoms at the following coordinates in the unit cell:



Pure CoO(II) has the NaCl structure with half of its cobalt sites and half of its oxygen sites vacant in such a way that each corresponding CoO(I) unit cell has two Co sites and two O sites vacant. Since there is no known preferable choice for any particular combination of the two vacant Co and O sites, we have 36 different possible combinations. In order to explain the experi-

<sup>21</sup> L. V. Azároff and M. J. Buerger, *The Powder Method in X-Ray Crystallography* (McGraw-Hill Book Co., Inc., New York, 1958).

<sup>22</sup> A. H. Compton and S. K. Allison, *X-rays in Theory and Experiment* (D. Van Nostrand Co., Inc., New York, 1935), 2nd ed.

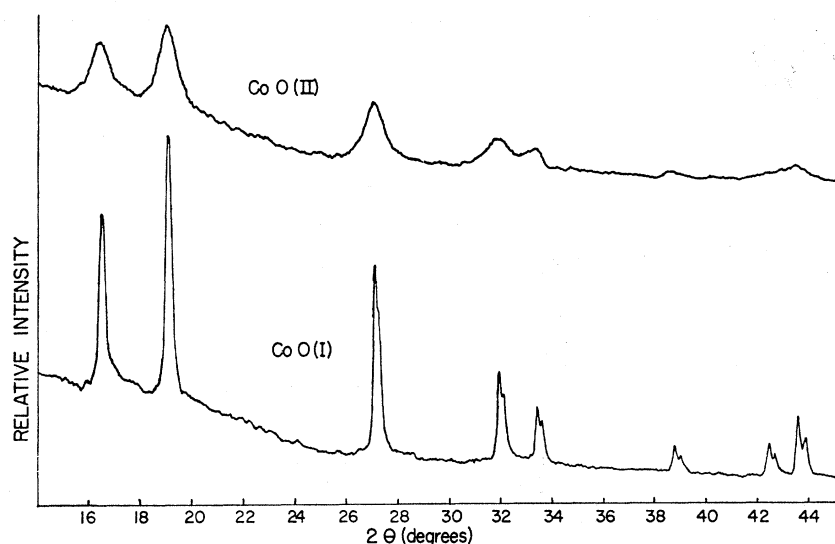


FIG. 11. X-ray diffraction patterns of CoO(I) and CoO(II) using Mo  $K\alpha_1$  and  $K\alpha_2$  x-ray, which was responsible for double peaks at large scattering angles.

mental data, it is necessary to assume that there is no long-range ordering greater than 50 Å, because calculations show that some additional lines in addition to the normal lines shown in Fig. 11 would result.

The relative intensities of the x-ray diffraction peaks for a powder sample are proportional to<sup>22</sup>

$$I = n[(1 + \cos^2 2\theta) / \sin 2\theta \sin \theta] |F_{hkl}|^2,$$

where  $F_{hkl} = \sum_j f_j \exp[2\pi i(hx_j + ky_j + lz_j)]$ ,  $h$ ,  $k$ ,  $l$  = Miller indices of a diffraction plane,  $f_j$  = atomic scattering factor of  $j$ th atom,  $x_j, y_j, z_j$  = coordinates of  $j$ th atom,  $n$  = number of equivalent planes, and  $\theta$  = diffraction angle. Using Mo  $K\alpha$  x ray of wavelength 0.7107 Å and the values of  $f_j$  from *International Tables of Crystallography*,<sup>23</sup> we calculated the relative intensities of the diffraction lines for CoO(I) and CoO(II). The results gave identical line positions and relative intensities for both CoO(I) and CoO(II) (see columns 1 and 2 in Table III). The calculations were carried out by a 7094 computer, and for the calculation of line positions and intensities of CoO(II) a microcrystal  $12 \times 12 \times 12$  times the unit cell specified above for CoO(I) was used, with the condition that no long-range ordering be permitted between vacancies in the microcrystal.

It is clearly seen that the experimental values in columns 4 and 5 are in good agreement with the theoretical values in column 2 based on our model. It is noticeable in Fig. 11 that the linewidths of CoO(II) are substantially broader than those of CoO(I). This can be understood if our sample consisted of ordered domains of sizes not greater than 50 Å. The disorientation between two adjoining grains (domains) renders

their scattering completely incoherent, so that they act as if they were separated. Since the domains are small in size, the x-ray diffraction lines are broadened by the size effect.<sup>24</sup> Failure to observe any additional x-ray lines for form II indicates that any short-range ordering within a domain cannot be identical to that in nearby domains. This is plausible since there are 36 different ways of arranging two Schottky defects in the perfect CoO(I) unit cell, specified above. Direct optical measurements of several particles of CoO(II) indicated that they were well defined, with an irregular shape having linear dimensions ranging between roughly  $10^{-3}$  and  $10^{-2}$  cm. This is consistent with the domain picture and appears to eliminate the possibility that small microcrystals caused the observed broadening in the x-ray pattern.

If each domain has different short-range ordering, Fe<sup>57</sup> ions in different domains will have different arrangements of nearest neighbors, and different charge asymmetries will produce different electric field gradients, each of which generally cause some splitting due to interaction with the nuclear quadrupole moment. The domain picture then can explain both the broadened x-ray lines and Mössbauer spectra for CoO(II). It should also be noted that asymmetries in the charge distributions, caused by the trapped electrons at different anion vacancies which adjoin the Fe<sup>3+</sup> ions, will be another source of electric field gradient, which also can account for the broadening of the hyperfine lines observed in CoO(II).

The calculated relative intensity distribution for a 25% cation-vacancy excess is shown in Table III, and it is in obvious disagreement with the experimental results. Therefore, a cation-vacancy model, either of the

<sup>23</sup> C. H. MacGillavry and G. D. Rieck, *International Tables of Crystallography* (The Kynoch Press, Birmingham, England, 1962), Vol. III, Chap. 3.3.

<sup>24</sup> A. Guinier, *X-ray Diffraction* (W. H. Freeman and Company, San Francisco, Calif., 1963).

low-concentration type or of the high-concentration type, is not consistent with our experimental results.

## VI. DISCUSSION

We proposed a model for cobaltous oxides based on the existence of two distinct structural forms. CoO(I) has the perfect NaCl structure, and CoO(II) has a NaCl structure with half of the cation and anion sites vacant. CoO(I,II) is a simple mixture of these two forms at 0°K, but is not a simple mixture at higher temperatures, where anions from clusters of form II disperse into form I.

Our proposed model was supported by the following observed properties:

(1) Stoichiometry measurements, which gave  $\text{CoO}_{1.00 \pm 0.05}$  for CoO(I), CoO(II), and CoO(I,II), show that all of our cobaltous-oxide samples had the correct chemical composition of one cobalt and one oxygen, and the composition of CoO(II) is consistent with a highly vacated structure, with equal numbers of cation and anion vacancies.

(2) Density measurements indicate that the density of CoO(II) is about half the value of CoO(I), which strongly supports the proposed picture of the CoO(II) structure.

(3) Mössbauer spectra which show pure  $\text{Fe}^{2+}$  lines for CoO(I), pure  $\text{Fe}^{3+}$  lines for CoO(II), and both 3+ and 2+ lines for the CoO(I,II) are in accord with our model and explain the mechanism by which charge compensation is achieved, i.e., anion vacancies can trap electrons resulting in  $\text{Fe}^{3+}$ .

(4) The observed oxidation property, that CoO(II) absorbs oxygen very rapidly but CoO(I) does not, also indicates a vacated structure for CoO(II).

(5) The irreversible conversion of CoO(II) to CoO(I) above 300°C in an inert atmosphere demonstrates that the metastable state of CoO(II) tends to convert to the stable state CoO(I), upon receiving sufficient thermal energy.

(6) The quenching of CoO(I,II) from high temperature, which enhanced the  $\text{Fe}^{2+}$  component of the Mössbauer pattern, indicates that strong stresses at elevated temperatures can cause the porous structure of form II to transform into form I.

(7) A much lower Mössbauer characteristic Debye temperature of 320°K for CoO(II) compared with 510°K for CoO(I) can be explained on the basis of our model, which would indicate only half of the covalent bonds per ion in CoO(II), as is found in CoO(I).

(8) While both pure CoO(I) and CoO(II) had decreasing  $f$  factors with increasing temperature, except for possible anomalous increases at the Néel temperatures, the area under the  $\text{Fe}^{3+}$  Mössbauer absorption line in CoO(I,II) increased with increasing temperature. This is attributed to an increasing number

of anion vacancies dispersed into form I. The anion-vacancy diffusion is not only supported by rapid oxygen absorption at room temperature in CoO(II), but also is supported by the  $\text{Fe}^{3+}$  Mössbauer patterns, which follow the  $f$  factor of CoO(I) at elevated temperatures instead of that of CoO(II), and had the same Néel temperature as form I instead of that of pure form II.

(9) X-ray diffraction patterns show identical line positions and relative intensities for pure CoO(I) and CoO(II), which is demanded by our model. The line broadening of CoO(II) patterns can be explained by assuming form II to consist of ordered domains of sizes not greater than 50 Å in CoO(II).

Wertheim<sup>1</sup> prepared a sample of CoO(I,II) which showed both  $\text{Fe}^{2+}$  and  $\text{Fe}^{3+}$  lines in its Mössbauer spectra, and he concluded that the  $\text{Fe}^{2+}$  line arose from stable states and  $\text{Fe}^{3+}$  was produced because the relaxation time for reaching electronic equilibrium following the emission of an Auger electron must be comparable to the  $\text{Fe}^{57m}$  nuclear lifetime of  $10^{-7}$  sec. The same kind of experiment was repeated and the same results as found by Wertheim were reported by Bhide and Shenoy,<sup>3</sup> who also found an increasing relative intensity for the  $\text{Fe}^{3+}/\text{Fe}^{2+}$  Mössbauer line with increasing temperature, and they proposed that the relaxation time for the conversion of  $\text{Fe}^{3+}$  to  $\text{Fe}^{2+}$  increases in CoO as the temperature is raised. We prepared CoO(I), which showed only  $\text{Fe}^{2+}$  lines over all temperatures (Fig. 6), and CoO(II), which showed only  $\text{Fe}^{2+}$  lines (Fig. 7). The fact that we could observe only  $\text{Fe}^{2+}$  over all temperatures for CoO(I) indicates that the observed  $\text{Fe}^{3+}$  is not connected with a temperature-dependent relaxation mechanism such as that proposed by Bhide and Shenoy.<sup>3</sup> Therefore, it is both unnecessary and inadequate to assume that  $\text{Fe}^{3+}$  lines observed in the Mössbauer spectra arise from Auger aftereffects.

Triftshäuser and Craig<sup>6,10</sup> also found no evidence for Auger aftereffects in CoO, using delayed-coincidence Mössbauer experiments. They showed that the relative intensity ratio  $I^{3+}/I^{2+}$  remains constant for all delay times studied. They proposed, however, that their data could be interpreted in terms of a small excess of cation vacancies in CoO. Our experimental results do not appear to be in harmony with this model.

Triftshäuser and Craig's proposal, accounting for their results on the basis of small deviations from ideal stoichiometry, is essentially based on three things: the electrical-conductivity measurements by Fisher and Tannhäuser,<sup>9</sup> absorber experiments, and x-ray determinations ascribable to the CoO(NaCl-type structure). The results of Fisher and Tannhäuser can at best be taken to establish that variations in stoichiometry are possible. We, of course, do not question this point, and our studies of the oxidation of CoO(II) clearly prove that excess oxygen is possible when this oxide is made.

The point which we would emphasize, however, is that our results lend support to the view that variations in stoichiometry are not, in fact, the reason why the two basic Mössbauer patterns [those corresponding to CoO(I) and CoO(II)] are observed. As shown in Sec. IV, the results of the TC absorber experiments are not confirmed by our experiments. As explained in detail in Sec. V, the same line positions and relative intensities of x-ray diffraction patterns are not generally unique in the determination of crystal structures involving large densities of defects.

Another possible explanation for the existence of  $\text{Fe}^{3+}$  in some experiments is recoil aftereffects.<sup>4,25</sup> The recoiling  $\text{Fe}^{57m}$  nucleus, whose recoil energy is of the order of 3 eV when the neutrino accompanying  $K$  capture is emitted, may cause a local rearrangement of the lattice which may produce complex spectra of the type observed in many hydrated crystals. Since CoO(I) and CoO(II) have been isolated and their properties can be explained by the existence of two forms of cobaltous oxide, it is unnecessary to assume recoil aftereffects for this material, even though some evidence of recoil aftereffects exists in other compounds, such as hydrated compounds.<sup>4</sup> We are planning additional experiments on the hydrated compounds to investigate in more detail the possibility that recoil aftereffects are the origin of the complex spectra seen in these materials.

Our model of two forms of cobaltous oxide has explained many experimental results better than any of the other models proposed so far, but we have some

unsettled points which should be investigated further. In order to explain the broad unresolved line seen in CoO(II) below the Néel temperature, we suggested that domain walls restrict the length of ordering. The existence and size of these domains were not convincingly established. Also, CoO(II) absorbed oxygen in the form of  $\text{CoO(II)} \cdot n\text{O}$ , but the limit of oxygen saturation was not determined.

Another important property which was not measured is the temperature required to achieve true thermodynamic equilibrium in experimentally accessible time intervals. While the large clusters of form II irreversibly transformed to form I above 600°K, smaller form-II clusters appeared stable at least to temperatures of 1000°K. This shows that the cation vacancies are immobile up to these temperatures, in contrast with the anion vacancies which are mobile above 200°K.

Many experiments on cobaltous oxide have been performed, especially in neutron-diffraction studies, conductivity studies, and x-ray studies. Now, it is likely that many of these experiments were carried out using CoO(I,II), and not the supposed CoO(I) with the perfect NaCl structure. There is also no reason why our proposed model may not be applied to other transition-metal oxides such as NiO. We think that it is likely that similar effects can be found in NiO, and experiments are planned along these lines.

#### ACKNOWLEDGMENTS

The authors wish to express their gratitude to Professor H. J. Yearian for the use of his x-ray diffractometer, and to Professor Grace and Professor Liedl for a stimulating discussion on this work.

<sup>25</sup> J. G. Mullen, Phys. Letters **15**, 15 (1965).